POLITECNICO DI TORINO
Repository ISTITUZIONALE

Seismic Performance of Bridges Depending on the DCFP Device Properties

Original
Seismic Performance of Bridges Depending on the DCFP Device Properties / Castaldo, P., Amendola, G.. - In: AIP CONFERENCE PROCEEDINGS. - ISSN 0094-243X. - ELETTRONICO. - 2849:(2023), pp. 1-4. (International Conference on Numerical Analysis and Applied Mathematics 2021, ICNAAM 2021 Sheraton Rhodes Resort, grc 2021) [10.1063/5.0163053].

Availability:
This version is available at: 11583/2984720 since: 2023-12-26T14:11:52Z

Publisher:
American Institute of Physics AIP

Published
DOI:10.1063/5.0163053

Terms of use:

This article is made available under terms and conditions as specified in the corresponding bibliographic description in the repository

Publisher copyright
AIP postprint/Author's Accepted Manuscript e postprint versione editoriale/Version of Record

(Article begins on next page)

17 November 2026

Seismic Performance of Bridges depending on the DCFP Device Properties

Paolo Castaldo[1, a)] and Guglielmo Amendola[1, b)]

[1]*Politecnico di Torino, Corso Duca degli Abruzzi, 10129, Turin, Italy*

[a)] Corresponding author: paolo.castaldo@polito.it
[b)] guglielmo.amendola@polito.it

Abstract. The present investigation examines how the properties of the double concave friction pendulum (DCFP) devices influence the seismic performance of isolated multi-span continuous deck bridges. The numerical simulations are carried out using an eight-degree-of-freedom model to reproduce the elastic behavior of the pier, associated to the assumption of both rigid abutment and rigid deck, and the non-linear velocity-dependent behavior of the two surfaces of the double concave friction pendulum isolators, under a set of natural records.

INTRODUCTION

The seismic isolation is one of the most used and efficient techniques able to improve seismic performance of both new or existing buildings [1] and infrastructures [2]. The main benefit to the bridges relates to significant reduction of forces transmitted from the deck to the piers under seismic event. In particular, the quantification of safety level of structures and road infrastructures [3] is a relevant research topic with special reference to areas subjected to high seismicity. For instance, different investigations focused on the analysis of seismic response of bridges equipped with isolator devices have been performed over the years [5-7], such as friction pendulum devices (FPS). The FPS bearings are able to make the natural period of the isolated bridge independent from the deck mass and allows significant energy dissipation under seismic motion thanks to friction on sliding surfaces [8]. The FPS devices can be realized with single or multiple concave sliding surfaces [9-10]. In particular, the use of double concave sliding surface friction pendulum devices (DCFP) have positive influence on the seismic response of isolated bridges as demonstrated by [11].

The present study investigates the effectiveness of the use of DCFP isolators to improve the seismic response of multi-span continuous bridges [12]. The structural response of the system under seismic excitations is analysed by means of an eight-degree-of-freedom (8-dof) model accounting for the reinforced concrete (RC) pier stiffness, the DCFP behaviour and the rigid RC abutment. The seismic action and related uncertainties are reproduced adopting a set of natural records. A non-dimensional parametric study is presented for some geometric configurations of the pier and of the DCFP isolators. The responses of the pier is monitored to determine effectiveness of the isolation system.

DYNAMIC BEHAVIOUR OF ISOLATED MULTI-SPAN CONTINUOUS BRIDGES: NON-DIMENSIONAL EQUATIONS OF MOTION

The structural behavior of the multi-span continuous deck bridge isolated with DPCF devices (e.g., isolated three-span continuous deck bridge) is reproduced by means of an 8-degree-of-freedom (8-dof) system as shown by Figure 1: 5 degrees of freedom for the elastic RC bridge pier, 2 degrees of freedom for the two sliders of the DPCF bearings and 1 degree of freedom for the mass of the rigid RC deck. The non-dimensional governing equations of motion of the system in Figure 1 can be expressed, in line with the proposal described in [13], as follows:

$$\ddot{\psi}_7(\tau)+\ddot{\psi}_6(\tau)+\ddot{\psi}_{p5}(\tau)+\ddot{\psi}_{p4}(\tau)+\ddot{\psi}_{p3}(\tau)+\ddot{\psi}_{p2}(\tau)+\ddot{\psi}_{p1}(\tau)+2\xi_d\dot{\psi}_7(\tau)+\frac{g}{2}\left[\frac{1}{R_{1p}}\frac{1}{\omega_d^{\,2}}\psi_7(\tau)+\frac{\mu_{1p}(\dot{\psi}_7)}{a_0}\mathrm{sgn}(\dot{\psi}_7)\right]+$$
$$+\frac{g}{2}\left[\frac{1}{R_{1a}}\frac{1}{\omega_d^{\,2}}\left(\sum_{i=1}^{5}\psi_{pi}(\tau)+\psi_6(\tau)+\psi_7(\tau)-\psi_8(\tau)\right)+\left(\frac{\mu_{1a}(\dot{\psi}_9)}{a_0}\right)\left(\mathrm{sgn}\left(\sum_{i=1}^{5}\dot{\psi}_{pi}(\tau)+\dot{\psi}_6(\tau)+\dot{\psi}_7(\tau)-\dot{\psi}_8(\tau)\right)\right)\right]=-\ell(\tau) \quad (1)$$

$$\lambda_{sp}\left[\ddot{\psi}_6(\tau)+\ddot{\psi}_{p5}(\tau)+\ddot{\psi}_{p4}(\tau)+\ddot{\psi}_{p3}(\tau)+\ddot{\psi}_{p2}(\tau)+\ddot{\psi}_{p1}(\tau)\right]-\frac{g}{2}\left[\frac{1}{R_{1p}}\frac{1}{\omega_d^{\,2}}\psi_7(\tau)+\frac{\mu_{1p}(\dot{\psi}_7)}{a_0}\mathrm{sgn}(\dot{\psi}_7)\right]+$$
$$+\left(\frac{1}{2}+\lambda_{sp}\right)g\left[\frac{1}{R_{2p}}\frac{1}{\omega_d^{\,2}}\psi_6(\tau)+\frac{\mu_{2p}(\dot{\psi}_6)}{a_0}\mathrm{sgn}(\dot{\psi}_6)\right]=-\lambda_{sp}\ell(\tau) \quad (2)$$

$$\lambda_{sa}\ddot{\psi}_8(\tau)-\frac{g}{2}\left[\frac{1}{R_{1a}}\frac{1}{\omega_d^{\,2}}\left(\sum_{i=1}^{5}\psi_{pi}(\tau)+\psi_6(\tau)+\psi_7(\tau)-\psi_8(\tau)\right)+\left(\frac{\mu_{1a}(\dot{\psi}_9)}{a_0}\right)\left(\mathrm{sgn}\left(\sum_{i=1}^{5}\dot{\psi}_{pi}(\tau)+\dot{\psi}_6(\tau)+\dot{\psi}_7(\tau)-\dot{\psi}_8(\tau)\right)\right)\right]+$$
$$+\left(\frac{1}{2}+\lambda_{sa}\right)g\left[\frac{1}{R_{2a}}\frac{1}{\omega_d^{\,2}}\psi_8(\tau)+\frac{\mu_{2a}(\dot{\psi}_8)}{a_0}\mathrm{sgn}(\dot{\psi}_8)\right]=-\lambda_{sa}\ell(\tau) \quad (3)$$

$$\lambda_{p5}\left[\ddot{\psi}_{p5}(\tau)+\ddot{\psi}_{p4}(\tau)+\ddot{\psi}_{p3}(\tau)+\ddot{\psi}_{p2}(\tau)+\ddot{\psi}_{p1}(\tau)\right]-2\xi_d\dot{\psi}_d(\tau)+2\xi_{p5}\lambda_{p5}\frac{\omega_{p5}}{\omega_d}\dot{\psi}_{p5}(\tau)+\frac{\lambda_{p5}\omega_{p5}^2}{\omega_d^2}\psi_{p5}(\tau)+$$
$$-\left(\frac{1}{2}+\lambda_{sp}\right)g\left[\frac{1}{R_{2p}}\frac{1}{\omega_d^{\,2}}\psi_6(\tau)+\frac{\mu_{2p}(\dot{\psi}_6)}{a_0}\mathrm{sgn}(\dot{\psi}_6)\right]=-\lambda_{p5}\ell(\tau) \quad (4)$$

$$\lambda_{p4}\left[\ddot{\psi}_{p4}(\tau)+\ddot{\psi}_{p3}(\tau)+\ddot{\psi}_{p2}(\tau)+\ddot{\psi}_{p1}(\tau)\right]-2\xi_{p5}\lambda_{p5}\frac{\omega_{p5}}{\omega_d}\dot{\psi}_{p5}(\tau)+2\xi_{p4}\lambda_{p4}\frac{\omega_{p4}}{\omega_d}\dot{\psi}_{p4}(\tau)-\lambda_{p5}\frac{\omega_{p5}^2}{\omega_d^2}\psi_{p5}(\tau)+\lambda_{p4}\frac{\omega_{p4}^2}{\omega_d^2}\psi_{p4}(\tau)=-\lambda_{p4}\ell(\tau) \quad (5)$$

$$\lambda_{p3}\left[\ddot{\psi}_{p3}(\tau)+\ddot{\psi}_{p2}(\tau)+\ddot{\psi}_{p1}(\tau)\right]-2\xi_{p4}\lambda_{p4}\frac{\omega_{p4}}{\omega_d}\dot{\psi}_{p4}(\tau)+2\xi_{p3}\lambda_{p3}\frac{\omega_{p3}}{\omega_d}\dot{\psi}_{p3}(\tau)-\lambda_{p4}\frac{\omega_{p4}^2}{\omega_d^2}\psi_{p4}(\tau)+\lambda_{p3}\frac{\omega_{p3}^2}{\omega_d^2}\psi_{p3}(\tau)=-\lambda_{p3}\ell(\tau) \quad (6)$$

$$\lambda_{p2}\left[\ddot{\psi}_{p2}(\tau)+\ddot{\psi}_{p1}(\tau)\right]-2\xi_{p3}\lambda_{p3}\frac{\omega_{p3}}{\omega_d}\dot{\psi}_{p3}(\tau)+2\xi_{p2}\lambda_{p2}\frac{\omega_{p2}}{\omega_d}\dot{\psi}_{p2}(\tau)-\lambda_{p3}\frac{\omega_{p3}^2}{\omega_d^2}\psi_{p3}(\tau)+\lambda_{p2}\frac{\omega_{p2}^2}{\omega_d^2}\psi_{p2}(\tau)=-\lambda_{p2}\ell(\tau) \quad (7)$$

$$\lambda_{p1}\ddot{\psi}_{p1}(\tau)-2\xi_{p2}\lambda_{p2}\frac{\omega_{p2}}{\omega_d}\dot{\psi}_{p2}(\tau)+2\xi_{p1}\lambda_{p1}\frac{\omega_{p1}}{\omega_d}\dot{\psi}_{p1}(\tau)-\lambda_{p2}\frac{\omega_{p2}^2}{\omega_d^2}\psi_{p2}(\tau)+\lambda_{p1}\frac{\omega_{p1}^2}{\omega_d^2}\psi_{p1}(\tau)=-\lambda_{p1}\ell(\tau) \quad (8)$$

with the following parameters denoting the mass ratios, the circular frequency of the isolated deck and of the *i*-th dof of the pier, the forces developed by the DCPS devices and the damping coefficient of the *i*-th dof of the pier:

$$\Pi_{\omega i}=\frac{\omega_{pi}}{\omega_d}\ ,\quad \Pi_{\lambda i}=\lambda_{pi}=\frac{m_{pi}}{m_d}\ ,\quad \Pi_{\lambda sa}=\lambda_{sa}\ ,\quad \Pi_{\lambda sp}=\lambda_{sp}\ ,\quad \Pi_{\mu 1a}(\dot{\psi}_9)=\frac{\mu_{1a}(\dot{\psi}_9)g}{a_0}\ , \quad (9),(10),(11),(12),(13)$$

$$\Pi_{\mu 1p}(\dot{\psi}_7)=\frac{\mu_{1p}(\dot{\psi}_7)g}{a_0}\ ,\quad \Pi_{\mu 2a}(\dot{\psi}_8)=\frac{\mu_{2a}(\dot{\psi}_8)g}{a_0}\ ,\quad \Pi_{\mu 2p}(\dot{\psi}_6)=\frac{\mu_{2p}(\dot{\psi}_6)g}{a_0}\ ,\quad \Pi_{\xi_{pi}}=\xi_{pi} \quad (14),(15),(16),(17)$$

The non-dimensional parameters $\Pi_{\mu 1a}$, $\Pi_{\mu 1p}$, $\Pi_{\mu 2a}$, $\Pi_{\mu 2p}$ depend on the velocities and are used as follows:

$$\Pi^*_{\mu 1a}=\frac{\mu_{1,\max,a}g}{a_0},\ \Pi^*_{\mu 1p}=\frac{\mu_{1,\max,p}g}{a_0},\ \Pi^*_{\mu 2a}=\frac{\mu_{2,\max,a}g}{a_0},\ \Pi^*_{\mu 2p}=\frac{\mu_{2,\max,p}g}{a_0} \quad (18),(19),(20),(21)$$

With reference to Figure 1, the peak response in terms of non-dimensional parameters (i.e., *peak deck response, peak isolator global response* and *peak displacement at the top of the pier*) can be expressed as:

$$\psi_{u_d}=\frac{u_{d,\mathrm{peak}}\omega_d^2}{a_0},\quad \psi_{x_d}=\frac{x_{d,\mathrm{peak}}\omega_d^2}{a_0}=\frac{(x_6+x_7)_{\mathrm{peak}}\omega_d^2}{a_0},\quad \psi_{u_p}=\frac{u_{p,\mathrm{peak}}\omega_d^2}{a_0}=\frac{(x_1+x_2+x_3+x_4+x_5)_{\mathrm{peak}}\omega_d^2}{a_0} \quad (22),(23),(24)$$

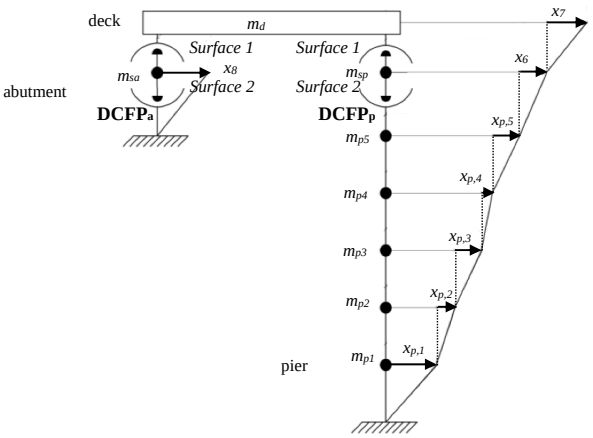

FIGURE 1. Representation of the 8-dof model of the bridge.

PARAMETRIC INVESTIGATION RESULTS

This section describes the results of parametric analysis of the bridge system isolated with DCFP bearings (Figure 1) considering a set of 30 ground motion records [14-15] and estimating the the mean value and dispersion of the *peak displacement at the top of the pier*. Specifically, the parametric analysis has been carried out considering the following structural properties: the parameters $\Pi_{\xi_d} = \xi_d$ and $\Pi_{\xi_p} = \xi_p$ are assumed, respectively, equal to 0% and 5%; the isolated bridge period T_d varies in the range 2s, 2.5s, 3s, 3.5s and 4s; the RC pier period T_p equal to 0.2s [11]; the five pier lumped masses have been considered equal and, so, $\Pi_\lambda = \lambda_p$ is equal to 0.1, 0.15 and 0.2 [11]; the two DCFP devices on the abutment and on the pier are identical (i.e., $\Pi^*_{\mu 1a} = \Pi^*_{\mu 1p} = \Pi^*_{\mu 1}$ as well as $\Pi_{\lambda sa} = \Pi_{\lambda sp} = \Pi_{\lambda s}$) and the mass ratio $\Pi_{\lambda s}$ is set equal to 0.005; R_1 / R_2 equal to 2, $\mu_{1,\max} / \mu_{2,\max}$ equal to 4, $\mu_{j,\max} / \mu_{j,\min}$ (with $j = 1,2$) equal to 3; the parameter $\Pi^*_{\mu 1}$ is assumed to vary in the range between 0 (no friction) and 2 (very high friction).

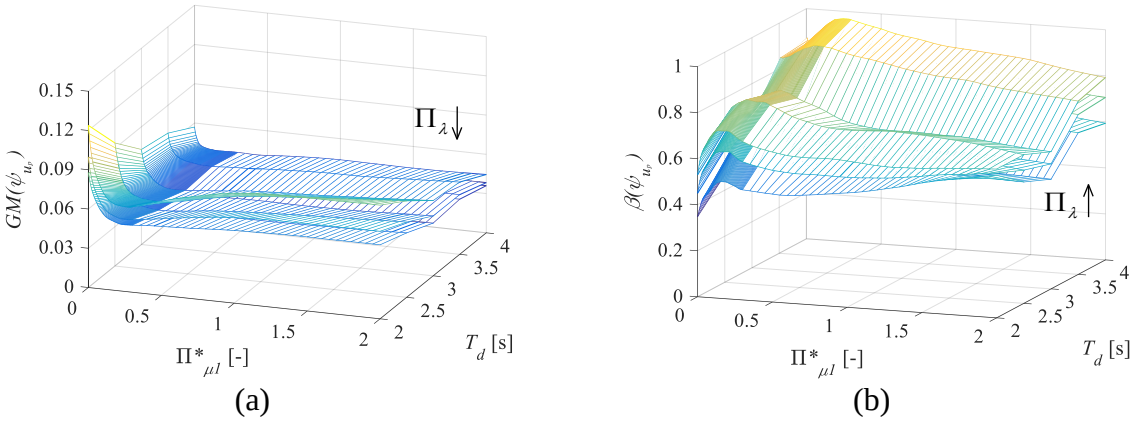

FIGURE 2. Normalized displacement of pier top vs. $\Pi^*_{\mu 1}$ and T_d: median value (a) and dispersion (b).

The non-dimensional parametric investigations have been carried out in Matlab-Simulink [16]. Figure 2 shows the statistics (*GM* and β values) of the non-dimensional peak response parameter considered. It is noteworthy that for very low $\Pi^*_{\mu 1}$ values, $GM\left(\psi_{u_p}\right)$ decreases by increasing $\Pi^*_{\mu 1}$, whereas it increases for high $\Pi^*_{\mu 1}$ values. Thus, there exists an optimal value of $\Pi^*_{\mu 1}$ such that the peak displacement of pier top is minimized. In addition, $GM\left(\psi_{u_p}\right)$ decreases with both increasing Π_λ and T_d. The dispersion shows a maximum value approximatively at the same value of $\Pi^*_{\mu 1}$ that gives the minimum of the geometric mean and increases with increasing both the mass ratio Π_λ and T_d.

CONCLUSIONS

This paper analyzes the seismic performance of multi-span continuous deck bridges isolated with DCFP devices. The results show that there exists an optimal value of sliding friction coefficient for each surface of the DCFP device able to minimize the pier response. This optimal value depends on the bridge and isolator properties.

REFERENCES

1. P. Castaldo, G. Alfano, "Seismic reliability-based design of hardening and softening structures isolated by double concave sliding devices", *Soil Dynamics and Earthquake Engineering*, **129**, 105930, 2020.
2. M.C. Constantinou, A. Kartoum, A.M. Reinhorn, P. Bradford, "Sliding isolation system for bridges", *Experimental study*, *Earthquake Spectra* **8**(3), 321-344, 1992.
3. D. Gino, P. Castaldo, G. Bertagnoli, L. Giordano, G. Mancini, "Partial factor methods for existing structures according to fib Bulletin 80: Assessment of an existing prestressed concrete bridge", *Structural Concrete*, **21**, 15-31, 2020.
4. R. Troisi, G. Alfano, "Towns as Safety Organizational Fields: An Institutional Framework in Times of Emergency", *Sustainability*, 11: 7025, 2019.
5. P. Tsopelas, M.C. Constantinou, S. Okamoto, S. Fujii, D. Ozaki, "Experimental study of bridge seismic sliding isolation systems", *Engineering Structures*, **18**(4), 301-310, 1996.
6. B.A. Olmos, J.M. Jara, J.M. Roesset, "Effects of isolation on the seismic response of bridges designed for two different soil types", *Bulletin of Earthquake Engineering*, **9**(2), 641-656, 2011.
7. M. Dicleli, S. Buddaram, "Effect of isolator and ground motion characteristics on the performance of seismic - isolated bridges", *Earthquake engineering & structural dynamics*, **35**(2), 233-250, 2006.
8. V.A. Zayas, S.S. Low, S.A. Mahin, "A simple pendulum technique for achieving seismic isolation", Earthquake *Spectra*, **6**, 317–33, 1990.
9. D.M. Fenz, M.C. Constantinou, "Behaviour of the double concave friction pendulum bearing", *Earthquake Engineering and Structural Dynamics*, **35**,1403-1424, 2006.
10. M.C. Constantinou, "Friction pendulum double concave bearings", *Technical report University of Buffalo NY*, October 29, 2004.
11. Y.S. Kim, C.B. Yun, "Seismic response characteristics of bridges using double concave friction pendulum bearings with tri-linear behavior", *Engineering Structures*, **29**, 3082-3093, 2007.
12. M.C. Kunde, R.S. Jangid, "Effects of pier and deck flexibility on the seismic response of isolated bridges", *Journal of Bridge Engineering*, **11**(1), 109-121, 2006.
13. P. Castaldo, G. Amendola, "Optimal DCFP bearing properties and seismic performance assessment in nondimensional form for isolated bridges", *Earthquake Engineering and Structural Dynamics*, 2021.
14. B. Palazzo, P. Castaldo, P. Della Vecchia, "Seismic reliability analysis of base-isolated structures with friction pendulum system", In 2014 IEEE Workshop on Environmental, Energy, and Structural Monitoring Systems Proceedings (pp. 1-6). IEEE.
15. P. Castaldo, B. Palazzo, G. Alfano, M.F. Palumbo, "Seismic reliability-based ductility demand for hardening and softening structures isolated by friction pendulum bearings", *Structural Control and Health Monitoring*, e2256, 2018.
16. Math Works Inc. MATLAB-High Performance Numeric Computation and Visualization Software. *User's Guide*. Natick: MA, USA, 1997.